

NMR ANALYSIS OF PROTEIN-SMALL MOLECULE INTERACTIONS

Reported by Thomas M. Anderson

April 16, 2007

INTRODUCTION

Advances in NMR technology over the last 20 years¹ have made information on solution structures of proteins increasingly available. High-resolution solution structures of proteins as large as 20-25 kDa are tractable in most cases,² and recent advances allowed Kay to solve the structure of an 82 kDa protein.³ These advances in NMR analysis of protein structure have made possible the study of protein-ligand interactions by NMR.⁴ From NMR data, detailed solution structures of protein-ligand complexes are accessible, and multiple methods for NMR-based analysis of protein-ligand interactions have been reported.⁴ Typically, proteins are labeled with NMR-active ¹⁵N and/or ¹³C nuclei to enhance backbone NMR signals. In addition, ²H-labels are often used to attenuate proton signals of the protein. Protein NMR spectra are analyzed in the presence and absence of ligand; based on ligand-induced changes in the NMR data, information about the location of ligand binding is obtained. The dissociation constant (K_d) for the ligand of interest is calculated directly from NMR data when the rate of ligand exchange is fast with respect to the NMR timescale.⁴ For ligands with slow exchange kinetics, conventional binding assays for K_d determination are more time-efficient.¹

CHEMICAL SHIFT MAPPING (CSM)

CSM compares protein spectra in the presence and absence of ligand.^{1,4} Ligand binding alters the local chemical environment in the binding site, resulting in chemical shift perturbations; these perturbations are correlated, or “mapped,” to the associated protein residues to determine the binding site. The orientation of the ligand in the binding site is determined from protein-ligand NOE correlations. A typical NMR experiment for CSM of protein binding sites is ¹⁵N-¹H heteronuclear single-quantum correlation (¹⁵N-HSQC),^{1,4-6} a two-dimensional experiment that correlates ¹⁵N nuclei with attached protons (one-bond ¹⁵N-¹H coupling). Thus, amide ¹⁵N-¹H correlations of ¹⁵N-labeled proteins are readily observed, and ¹⁵N-HSQC CSM is accomplished by correlating observed chemical shift perturbations in ¹⁵N-¹H cross-peaks to protein residues.

STRUCTURE-ACTIVITY RELATIONSHIPS (SAR) BY NMR

SAR by NMR is a CSM approach to ligand optimization developed by Fesik and coworkers at Abbott Laboratories.⁶ In this technique, two ligands occupying distinct, proximal sites are identified by ¹⁵N-HSQC CSM. Optimization of the two ligands and subsequent covalent tethering of the two “fragments” leads to a ligand which typically exhibits improved binding over either of the first two. While this approach requires the researcher to have some structural information on the target protein, it

offers several potential advantages. First, ligands that bind to two distinct binding sites should have higher specificity than those which only target one site. Second, because the protein is ^{15}N -labeled, large excess of the ligand may be used, and K_d values may be calculated directly from NMR data with no background signal from the ligand.⁴ Thus, NMR screening can identify weak-binding ligands ($K_d > 1$ mM), obviating lengthy synthesis of the initial library. NMR structures provide a basis for rational linker design, further reducing the amount of synthesis required for ligand optimization. Finally, targeting two separate binding sites decreases the probability of drug resistance because two sites must undergo mutation for resistance to develop.

In a proof-of-concept experiment,⁶ Fesik and coworkers used SAR by NMR to identify ligands optimized for binding to the FK506-binding protein (FKBP). Initially, unoptimized ligands were identified by recording ^{15}N -HSQC spectra of ^{15}N -labeled FKBP in the presence and absence of ligands. The first library screen identified pipecolic ester **1** (Figure 1, $K_d = 2$ μM) from chemical shift perturbations in the ^{15}N -HSQC spectrum upon addition of **1**. To identify a second, proximal binding site,

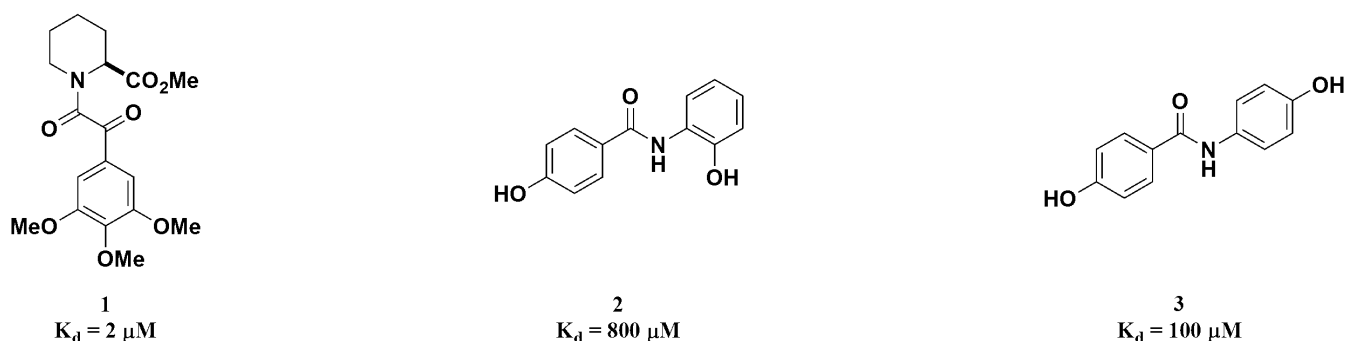
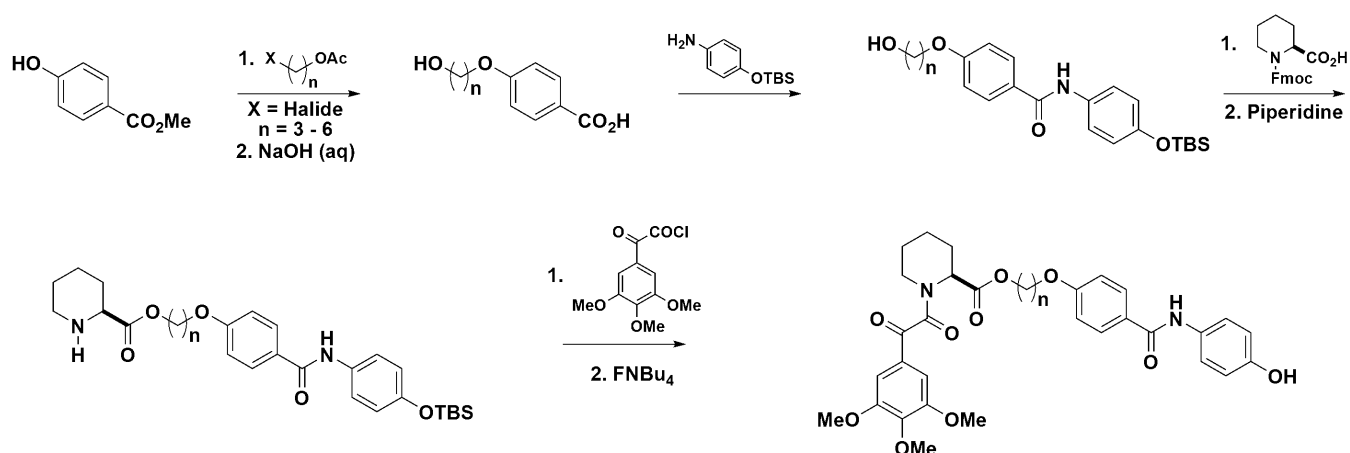


Figure 1. FKBP ligands identified by ^{15}N -HSQC screening.

^{15}N -HSQC spectra of FKBP and 2.0 mM **1** were recorded in the presence of compounds from a second library. This second screen identified **2** (Figure 1), which bound to FKBP with $K_d = 800$ μM . Protein-ligand NOESY correlations established proximity of the two binding sites. SARs for **2** were investigated by variations in hydroxyl substitution patterns of the phenyl moieties, and **3** (Figure 1) showed improved binding to FKBP with $K_d = 100$ μM .

To further enhance binding of the two ligands, Fesik envisioned that covalently tethering the two ligands would create a cooperative binding effect. A series of tethered ligands of variable linker length were synthesized (Scheme 1). The optimal tether length was $n = 3$, resulting in a ligand with $K_d = 19$ nM. This new ligand bound to the same site as compounds **1** and **2**, as determined from protein-ligand NOESY correlations.



Scheme 1. Synthesis of tethered ligands for FKBP.

TARGETING ANTIAPOPTOTIC B CELL LYMPHOMA-2 (BCL-2) PROTEINS

Having demonstrated the feasibility of SAR by NMR, Fesik applied the technique toward identifying inhibitors of antiapoptotic Bcl-2 proteins.⁷⁻¹⁰ These proteins, which are overexpressed in several human cancer cell lines, include Bcl-2, Bcl-X_L, Bcl-w, Mcl-1, and A1.⁷⁻⁸ In healthy cells, proapoptotic Bcl proteins such as Bad, Bak, Bim, and others sequester the antiapoptotic Bcl counterparts, allowing for normal cell death. Using SAR by NMR, Fesik and coworkers sought to optimize ligands for Bcl-X_L.

A screen of commercially available and proprietary compounds identified **4** (Figure 2),⁸ which binds to Bcl-X_L with $K_d = 300 \mu\text{M}$. This screen revealed that the carboxyl group of **4** was crucial for effective binding, as compounds lacking the carboxyl were less active. In the presence of **4**, compound **5**

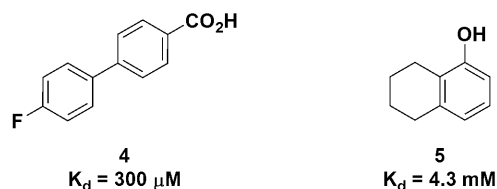


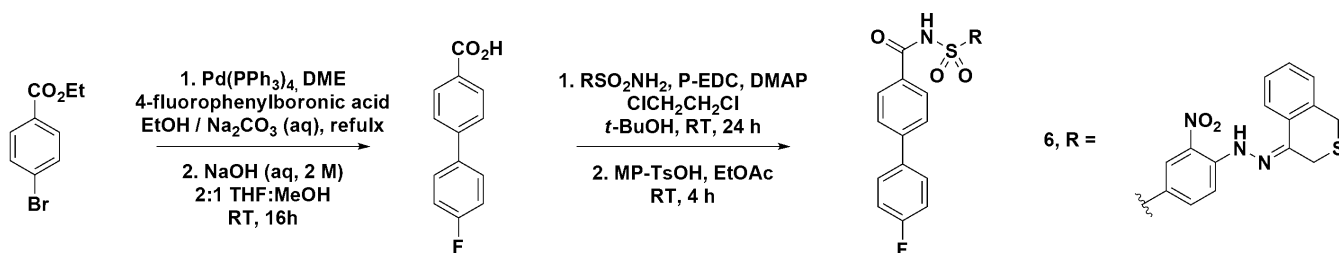
Figure 2. Bcl-X_L ligands identified by ¹⁵N-HSQC screening.

was found to bind to a proximal binding site ($K_d = 4.3 \text{ mM}$). NMR structures of the Bcl-X_L/**4/5** complex revealed two hydrophobic pockets separated by the Phe97 side chain. The binding sites for **4** and **5** correspond to the region of the protein for binding Bad and Bak.⁷ For ease of reference, the binding sites for **4** and **5** will be referred to as Sites 1 and 2, respectively.

To preserve the acidic Site 1 functionality and allow for fragment linking, an acylsulfonamide tether was employed (acylsulfonamides typically have $\text{p}K_a$ 3-5). To test the utility of the acylsulfonamide as a carboxyl isostere, the methyl acylsulfonamide analog of **4** was synthesized via the general route shown in Scheme 2. Its activity ($K_d = 320 \mu\text{M}$) is similar to that of **4**. An acylsulfonamide library was

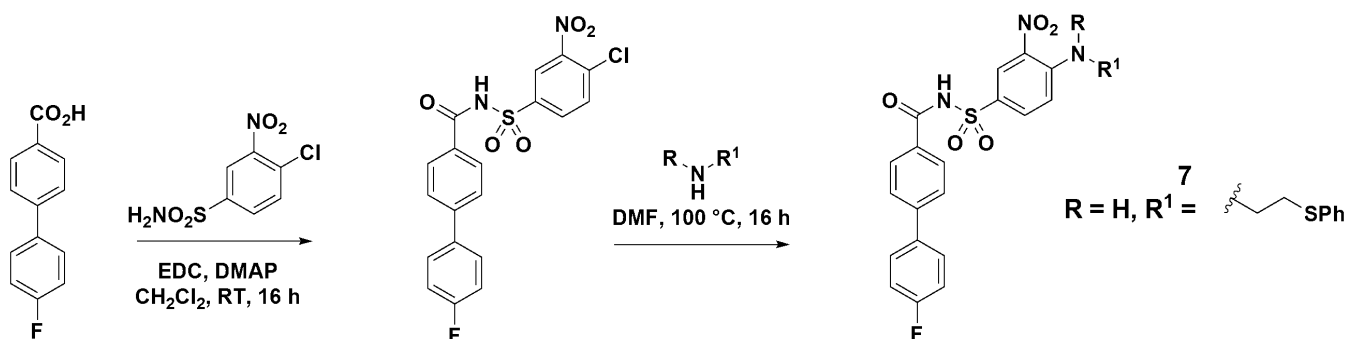
synthesized (Scheme 2), and the nitrophenyl acylsulfonamide **6** was identified as the most promising hit. Because the exchange rate of **6** was slow with respect to the NMR timescale, the K_d was not calculated from NMR data, and a fluorescence polarization assay was used to determine an inhibition constant (K_i) of 0.25 μM . Analysis of the NMR-derived structure of the Bcl-X_L/**6** complex reveals that the acylsulfonamide bridges over Phe97 as desired. Furthermore, the orientation of the nitrophenyl of **6** allows for potential π -stacking with Tyr194 and Phe97, possibly contributing to the enhanced binding.

Scheme 2. Acylsulfonamide library synthesis.



To further optimize Site 2 binding, a library of nitrophenyl acylsulfonamides was synthesized by the general route shown in Scheme 3. From **4**, the corresponding 4-chloro-3-nitrophenyl acylsulfonamide was prepared via coupling with 4-chloro-3-nitrophenylsulfonamide. Nucleophilic aromatic substitution of primary and secondary amines yielded 125 compounds, of which **7** was

Scheme 3. Synthesis of nitrophenyl acylsulfonamide library.



identified with improved affinity for Bcl-X_L ($K_i = 36$ nM). From the NMR-derived structure of **7** bound to Bcl-X_L, the position of the thiophenyl moiety allows for enhancement of the putative π -stacking with Phe97 and Tyr194. Thus, starting from two weak-binding ligands (**4**, $K_d = 300$ μM and **3**, $K_d = 4.3$ mM), SAR by NMR was successful in identifying a nanomolar inhibitor of Bcl-X_L. However, **7** had reduced affinity for Bcl-X_L in the presence of 1% human serum ($K_i = 2.5$ μM). Human serum albumin (HSA) was identified as a competitive binder for **7**.

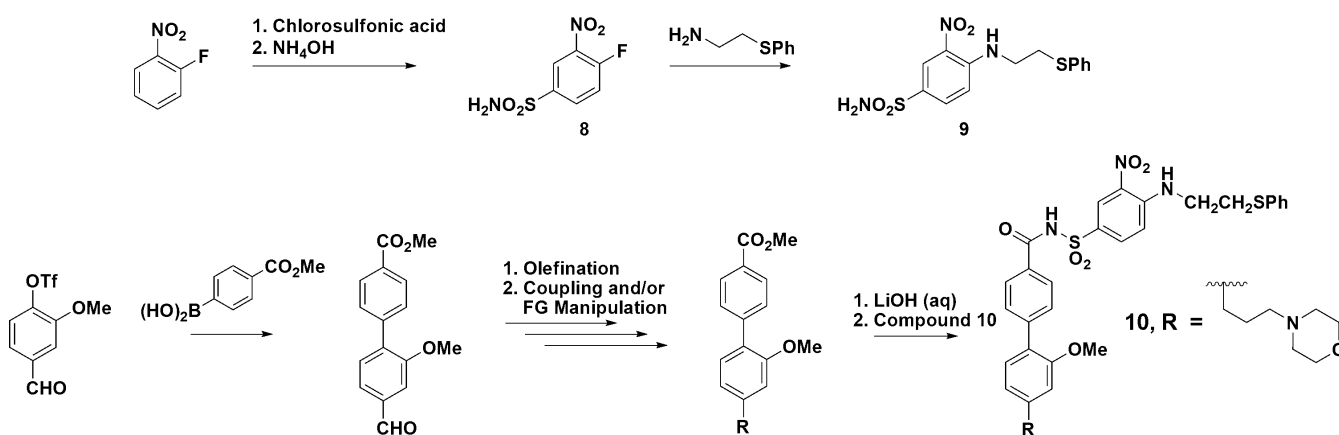
REDUCING AFFINITY FOR HUMAN SERUM ALBUMIN

To maintain the potential clinical relevance of **7**, the researchers sought to modify the scaffold to decrease affinity for HSA while maintaining affinity for Bcl-X_L.⁹ The NMR-derived structure of the

HSA/7 complex showed that the biphenyl moiety interacted with HSA in a deep hydrophobic pocket that was inaccessible to solvent.^{7,9} However, the analogous Site 1 of Bcl-X_L was observed to be solvent-accessible. Further, while the HSA binding site did not appear capable of accommodating any further steric bulk at the biphenyl, the hydrophobic Site 1 of Bcl-X_L appeared to have space for extra substituents on the biphenyl. The binding mode of the 2-(phenylthio)-aminoethyl moiety was also examined. The HSA binding site was hydrophobic and solvent-inaccessible at this position, whereas Site 2 of Bcl-X_L was solvent-accessible and thus would allow for functionalization at the ethyl carbons.

Based on these observations, a library of functionalized biphenyl compounds was synthesized (Scheme 4) to assess the effectiveness of altering the steric environment and polarity of the biphenyl. Consistent with the observation of the deep hydrophobic pocket of HSA, charged R groups were most effective for reducing HSA affinity. Compound **10** was found to bind to Bcl-X_L with $K_i = 0.01 \mu\text{M}$, with $K_i = 0.6 \mu\text{M}$ in the presence of Bcl-X_L and 1% HSA. The morpholine moiety was then incorporated in a

Scheme 4. Synthesis of biaryl derivatives of decreased HSA affinity.

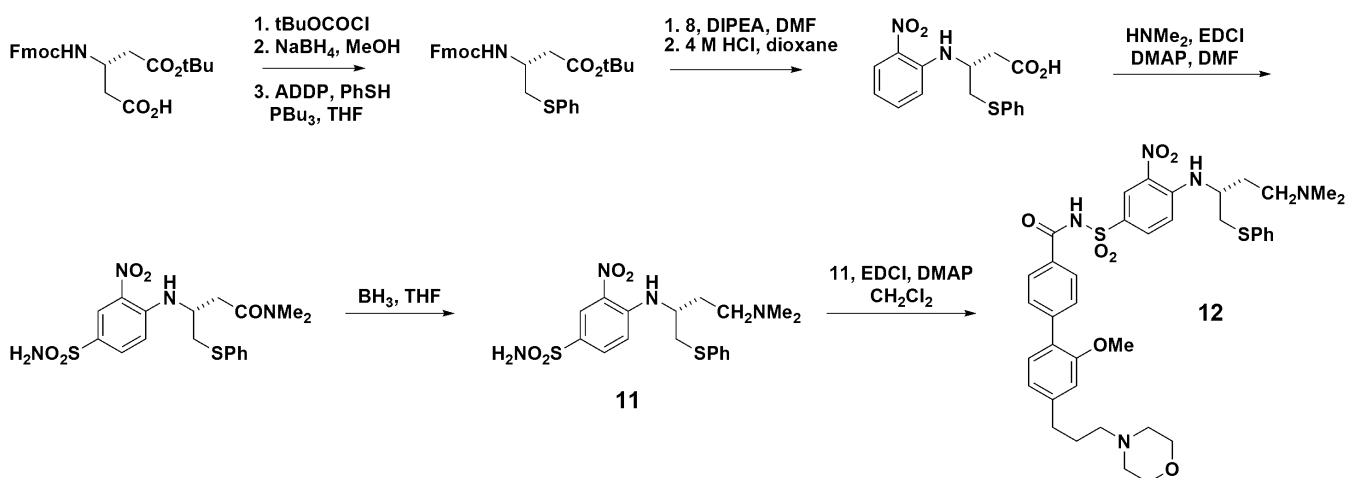


synthesis (Scheme 5) to derivatize the α -methylene of the 2-(phenylthio)-aminoethyl group. While this introduced a chiral ligand, the *R* enantiomers were found to have higher Bcl-X_L affinity, consistent with the position of the diastereotopic methylene protons in the Bcl-X_L/7 complex. Compound **12** showed lower affinity for HSA, with $K_i = 0.36 \mu\text{M}$ in the presence of Bcl-X_L and 10% HSA. Surprisingly, **12** inhibited Bcl-X_L with $K_i = 8 \text{ nM}$, an improvement of two orders of magnitude over **10**.

OPTIMIZING BINDING FOR BOTH BCL-X_L AND BCL-2

Given the therapeutic potential of targeting both Bcl-X_L and Bcl-2, Fesik next sought to design a compound for binding to Bcl-2 without a decrease in Bcl-X_L affinity.¹⁰ Bcl-2 and Bcl-X_L differ by only three residues in the binding site under consideration. The key difference, which Fesik exploited, was the presence of Met108 in Bcl-2, which had greater conformational flexibility in the Site 1 groove than the corresponding Leu108 in Bcl-X_L. The conformational flexibility of Met108 allowed access to a deep

Scheme 5. Synthesis of Bcl-X_L ligands with decreased HSA affinity.



hydrophobic groove of Bcl-2 that was not observed in the structure of Bcl-X_L. NMR-based structural studies of a ligand containing a Site 1 phenethyl-substituted benzothiazole docked with Bcl-2 and Bcl-X_L revealed that the phenethyl moiety occupied the hydrophobic groove of Bcl-2 while maintaining a surface orientation on the face of the Bcl-X_L binding site. Thus, Fesik envisioned that the Site 1 fragment could be modified to enhance Bcl-2 binding without reduction of affinity for Bcl-X_L.

Fesik had previously identified **13**,⁹ containing a Site 1 *N*-phenyl piperidine in place of the biphenyl, which inhibited Bcl-2 with $K_i = 67$ nM. However, a screen of several analogous *N*-phenyl compounds revealed that a piperazine ring allowed for better Bcl-2 affinity while maintaining Bcl-X_L affinity. Figure 3 shows four representative examples from this library. The *N*'-benzyl piperazine **14** was

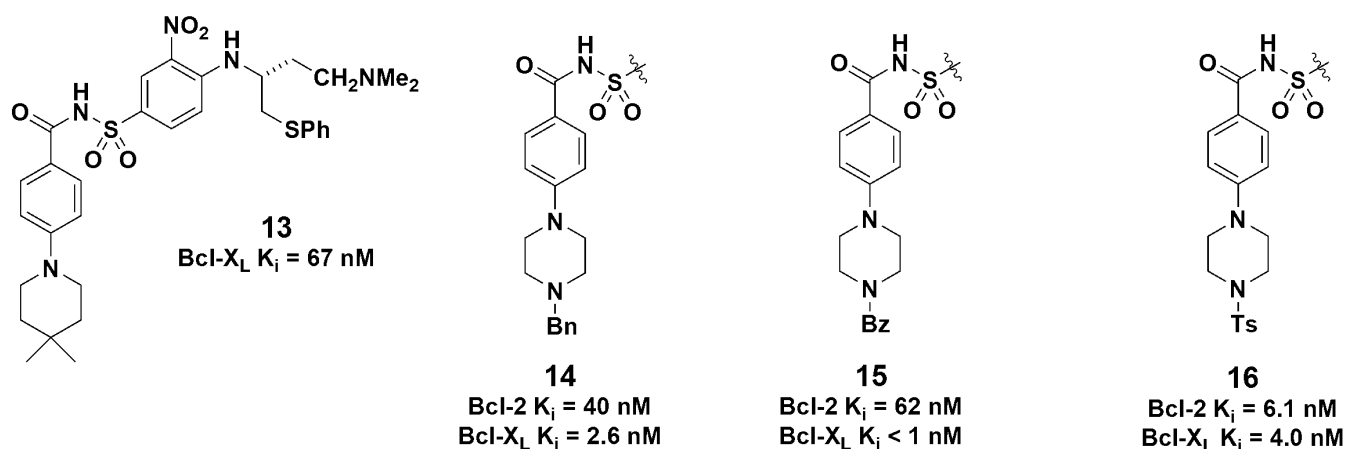
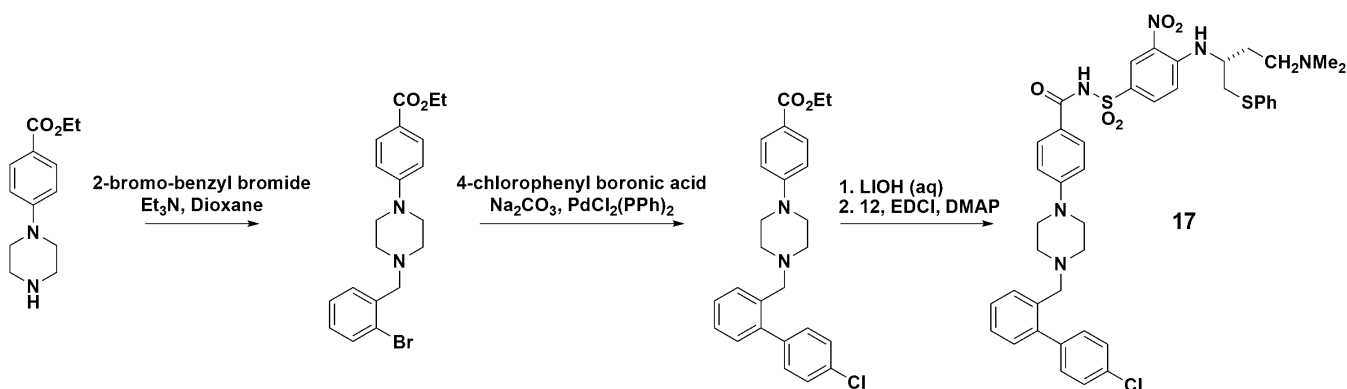


Figure 3. Comparison of **13** with substituted *N*-phenylpiperazines.

chosen for further elaboration, and a library was synthesized which contained a variety of substituted benzyl groups. Compound **17**, whose synthesis is shown in Scheme 6, was the most active library member with $K_i < 1$ nM for Bcl-2 and $K_i < 0.5$ nM for Bcl-X_L.

Scheme 6. Synthesis of optimized ligand for Bcl-2 and Bcl-X_L.



OTHER NMR METHODS FOR ANALYZING INTERMOLECULAR INTERACTIONS

While SAR by NMR represents the use of NMR as a drug discovery tool, NMR techniques have been developed and applied for studying protein-ligand interactions in other contexts.⁴ Nishida has applied an NOE-based CSM technique to identify the binding site for fibrillar collagen (FC) binding to a collagen-binding protein (CBP).¹¹ The collagen protein contained no isotope labels, while the CBP contained ^{15}N - and ^2H isotope labels. Amide deuterons were exchanged in H_2O to allow for observation of ^{15}N - ^1H correlations. In an experiment analogous to the standard NOESY technique, saturation of the aliphatic ^1H resonances allowed for NOE correlations to develop at the FC-CBP binding interface. After the saturation pulse, a ^{15}N -HSQC spectrum was obtained. ^{15}N -HSQC cross-peak intensities decreased for some residues (relative to the complex with no saturation pulse). Subsequent mapping of the affected residues revealed a contiguous binding domain on the CBP.

Carlomagno and coworkers have developed an NMR-based method¹² for analysis of competitive binding of two weak-binding ligands. Epothilones and taxanes competitively bind to microtubules, but binding of these compounds with free tubulin has not been characterized due to the weak nature of these interactions. A NOESY spectrum of a mixture of the taxane baccatin III (**18**, Figure 4), epothilone A (**19**), and tubulin gives rise to cross-peaks between epothilone A and baccatin III which are not observed in the absence of tubulin.

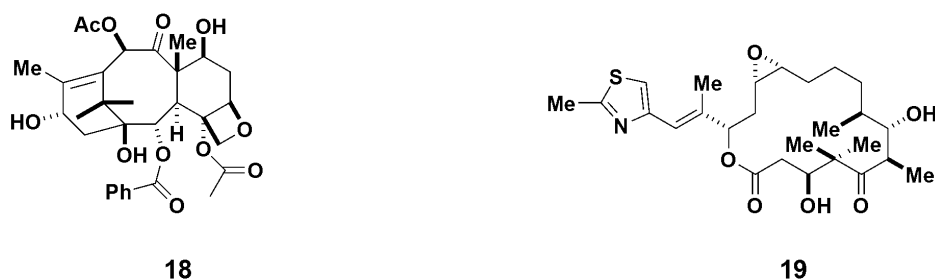


Figure 4. Baccatin III and Epothilone A.

CONCLUSION

Advances in NMR spectroscopy have provided powerful tools for both structural analysis and structure-activity studies. While SAR by NMR is a relatively new technique, it can be utilized to discover potent protein ligands and potential drug leads. Through the use of SAR by NMR, a new drug lead targeting antiapoptotic Bcl proteins was developed. At the time of publication,⁷ this ligand was 2-3 orders of magnitude more active than any previously reported Bcl-X_L or Bcl-2 inhibitor. While this discovery illustrates the potential of CSM for identifying and optimizing protein-ligand binding, the NMR techniques discussed herein are not limited to study of protein-ligand interactions and could be extended to study other types of intermolecular interactions.

REFERENCES

- 1) Cavanagh, J.; Fairbrother, W. J.; Palmer, W. G. III; Rance, M.; Skelton, N. J. Protein NMR Spectroscopy: Principles and Practices, 2nd Ed. Academic Press, San Diego, **2006**.
- 2) Kay, L. E.; Gardner, K. H. *Curr. Opin. Struct. Biol.* **1997**, *7*, 722-731.
- 3) Tugarinov, V.; Choy, W.-Y.; Orekhov, V. Y.; Kay, L. E. *Proc. Natl. Acad. Sci. USA* **2005**, *102*, 622-627.
- 4) Pellechia, M. *Chem. Biol.* **2005**, *12*, 961-971.
- 5) Görlach, M.; Wittekind, M.; Beckman, R. A.; Mueller, L.; Dreyfuss, G. *EMBO J.* **1992**, *11*, 3289-3295
- 6) Shuker, S. B.; Hajduk, P. J.; Meadows, R. P.; Fesik, S. W. *Science* **1996**, *274*, 1531-1534.
- 7) Oltersdorf, T.; Elmore, S. W.; Shoemaker, A. R.; Armstrong, R. C.; Augeri, D. J.; Belli, B. A.; Bruncko, M.; Deckwerth, T. L.; Dinges, J.; Hajduk, P. J.; Joseph, M. K.; Kitada, S.; Korsmeyer, S. J.; Kunzer, A. R.; Letai, A.; Li, C.; Mitten, M. J.; Nettesheim, D. G.; Ng, S.-C.; Nimmer, P. M.; O'Connor, J. M.; Oleksijew, A.; Petros, A. M.; Reed, J. C.; Shen, W.; Tahir, S. K.; Thompson, C. B.; Tomaselli, K. J.; Wang, B.; Wendt, M. D.; Zhang, H.; Fesik, S. W.; Rosenberg, S. H. *Nature* **2005**, *435*, 677-681.
- 8) Petros, A. M.; Dinges, J.; Augeri, D. J.; Baumeister, S. A.; Betebenner, D. A.; Bures, M. G.; Elmore, S. W.; Hajduk, P. J.; Joseph, M. K.; Landis, S. K.; Nettesheim, D. G.; Rosenberg, S. H.; Shen, W.; Thomas, S.; Wang, X.; Zanze, I.; Zhang, H.; Fesik, S. W. *J. Med. Chem.* **2006**, *49*, 656-663.
- 9) Wendt, M. D.; Shen, W.; Kunzer, A.; McClellan, W. J.; Bruncko, M.; Oost, T. K.; Ding, H.; Joseph, M. K.; Zhang, H.; Nimmer, P. M.; Ng, S.-C.; Shoemaker, A. R.; Petros, A. M.; Oleksijew, A.; Marsh, K.; Bauch, J.; Oltersdorf, T.; Belli, B. A.; Martineau, D.; Fesik, S. W.; Rosenberg, S. H.; Elmore, S. W. *J. Med. Chem.* **2006**, *49*, 1165-1181.
- 10) Bruncko, M.; Oost, T. K.; Belli, B. A.; Ding, H.; Joseph, M. K.; Kunzer, A.; Martineau, D.; McClellan, W. J.; Mitten, M.; Ng, S.-C.; Nimmer, P. M.; Oltersdorf, T.; Park, C.-M.; Petros, A. M.; Shoemaker, A. R.; Song, X.; Wang, X.; Wendt, M. D.; Zhang, H.; Fesik, S. W.; Rosenberg, S. H.; Elmore, S. W. *J. Med. Chem.* **2007**, *50*, 641-662.
- 11) Nishida, N.; Sumikawa, H.; Sakakura, M.; Shimba, N.; Takahashi, H.; Terasawa, H.; Suzuki, E. I.; Shimada, I. *Nat. Struct. Biol.* **2003**, *10*, 53-58.
- 12) Sánchez-Pedregal, V. M. Reese, M. Meiler, J. Blommers, M. J. J. Griesinger, C. Carlomagno, T. *Angew. Chem. Int. Ed.* **2005**, *44*, 4172-4175.